Effect of placement of droop based generators in distribution network on small signal stability margin and network loss

Dheer, D.K. ; Doolla, S.; Bandyopadhyay, S. ; Guerrero, Josep M.

Published in:
International Journal of Electrical Power & Energy Systems

DOI (link to publication from Publisher):
10.1016/j.ijepes.2016.12.014

Publication date:
2017

Document Version
Early version, also known as pre-print

Effect of placement of droop based generators in distribution network on small signal stability margin and network loss

D.K. Dheer, S. Doolla,, S. Bandyopadhyay, Josep M. Guerrero
a Department of Energy Science and Engineering, Indian Institute of Technology Bombay, Powai, Mumbai 400076, India
b Department of Energy Technology, Power Electronic Systems, Aalborg University, 9220 Aalborg, Denmark

Abstract

Optimal location of distributed generators (DGs) in a utility-connected system is well described in literature. For a utility-connected system, issues related to small signal stability with DGs are insignificant due to the presence of a very strong grid. Optimally placed sources in utility connected microgrid system may not be optimal/stable in islanded condition. Among others issues, small signal stability margin is on the fore. The present research studied the effect of location of droop-controlled DGs on small signal stability margin and network loss on an IEEE 33-bus distribution system and a practical 22-bus radial distribution network. A complete dynamic model of an islanded microgrid was developed. From stability analysis, the study reports that both location of DGs and choice of droop coefficient have a significant effect on small signal stability and transient response of the system. For multi-objective optimization of the DG network, Pareto fronts were identified and the non-dominated solutions found with two and three generators. Results were validated by time domain simulations using MATLAB.

Keywords: Islanded microgrid, droop control, small signal stability margin.

1. Introduction

Growing environmental concerns competitive energy policies has led to the decentralization of power generation. Installations of distributed generators (DGsphotovoltaic, wind, etc.) are expected to increase worldwide in the next decade [1]. Due to their location being close to consumers, DGs provide better power in terms of quality and reliability [2]. Controllable DGs along with controllable loads present themselves to the upstream network as microgrid. Microgrids when operating in grid-connected mode provide/draw power

based on supply/demand within. In islanded mode (when not connected to the main grid), microgrids operate as an independent power system [2].

The optimality in placement of a DG is decided by the owner based on the availability of primary resource, site, and climatic conditions. Thus, choosing an inappropriate location may result in losses and fall in power quality. Literature has widely addressed optimal placement of DGs in a network based on objective functions of energy/power loss minimization, cost minimization, voltage deviation minimization, profit maximization, loadability maximization, etc [3]. Different approaches, methods, and optimization techniques for DG siting and sizing are presented in [3]-[9].

DG siting and sizing is a multi-objective optimization problem classifiable into two groups. The first group focuses on economics of the system [9]-[17]. With respect to islanded microgrids, minimization of total annual energy losses and cost of energy for distributed generation is an area of much interest to investors [10]. One study [9] presented a multi-objective optimization problem of minimization of photovoltaic, wind generator and energy storage investment cost, expectation of energy not supplied, and line loss. Economic and environmental restrictions for a microgrid are outlined in [11]. Operation cost (local generation cost and grid energy cost) minimization is presented in [12]. An optimization problem considering operation cost and emission minimization is presented in [13]. Economic dispatch problem in a hybrid, droop-based microgrid is presented in [14].

The second group focuses on the optimal design of a microgrid based on technical parameters such as network losses, maximum loadability, voltage profile, reactive power, power quality, and droop setting. The assessment of maximum loadability for a droop-based islanded microgrid is presented in [18]-[20] considering reactive power requirements and various load types. A decision-making program for load procurement in a distribution network is presented in [21] based on uncertainty parameters like electricity demand, local power investors, and electricity price. Optimal setting of droop to minimize the cost of wind generator is presented in [22]. One wind-generation study combined economics and stability issues due to uncertainty (volatility) and its effect on small signal stability [23]-[24]. This study of small signal stability in droop-based islanded microgrids is thus worthy in the context of potential benefits of optimal DG placement to grid managers.

A microgrid may present as much complexities as a conventional power system. When connected to a grid, these optimally placed and sized DGs (inverter-based) operate in current control mode, feeding maximum power to

the network. When a grid is not available, these DGs shift to droop control mode for effective power sharing.

Two important aspects of an islanded microgridload sharing and stabilityare widely addressed in literature. A higher droop in these DGs is desired for better power sharing and transient response [25]-[28]. Higher droop and stability margin improves the transient response of the system and hence power sharing among the sources [28]]. Inappropriate settings of droop value may cause a power controller to operate at low frequency mode and fall into an unstable region[29]-[31]. Stability of islanded microgrids [25]-[27] is a growing operational challenge. A grid-connected system optimized for DG sizing and siting may be vulnerable to small signal stability when islanded.

The impact of optimal DG placement on enhancement of small signal stability margin and loss minimization is investigated on a standard IEEE 33-bus distribution system and a practical 22-bus radial distribution network of a local utility. The rest of the paper is organized as follows: Section 2 presents a description of the system considered and the mathematical model designed for stability studies. Eigen value analysis and identified Pareto fronts are presented in Section 3. Validation of Eigen value analysis by time domain simulation is presented in Section 4, followed by conclusions of the study in Section 5.

2. System Description and Mathematical Modeling

Microgrids integrated with renewable energy sources through voltage source inverters (VSIs), together with loads and interconnecting lines, were considered for the present study. An IEEE 33-bus radial distribution system (Fig. 1) and a 22-bus practical radial distribution network of Andhra Pradesh Eastern Power Distribution Company Limited (APEPDCL) (Fig. 2) were considered.

2.1. System State Space Equation

The modeling of VSIs, line, and load in *d-q* axis reference frame for small signal stability is defined in [32]. Equation (1) is the overall state space (matrix) equation for the total system under consideration. For the IEEE 33-bus system, the size of matrix A_{MG} with two generators is 152×152, which includes 26 states of DGs, 62 states of lines, and 64 states of loads. With three generators, the size of A_{MG} is 165×165 (39 states of DGs, 62 states of lines, and 64 states of loads). Similarly, for the 22-bus practical radial

distribution network of APEPDCL, the size of A_{MG} with three generators is 121×121 (39 states of DGs, 40 states of lines, and 42 states of loads).

$$\begin{bmatrix} \Delta\dot{X}_{DG} \\ \Delta I_{DQ_{Line}} \\ \Delta I_{DQ_{Load}} \end{bmatrix} = A_{MG} \begin{bmatrix} \Delta X_{DG} \\ \Delta I_{DQ_{Line}} \\ \Delta I_{DQ_{Load}} \end{bmatrix} \tag{1}$$

2.2. Loss calculation

Consider a line of impedance $(R + jX)\ \Omega$ connected between two nodes through which current I_i is flowing. This current (I_i) can be expressed as:

$$I_i = I_d \pm jI_q \tag{2}$$

Real power loss in the line can be calculated using :

$$P_{loss,i} = I_i^2 \times R \tag{3}$$

where, $I_i^2 = I_d^2 + I_q^2$. Total real power loss of the network containing n lines is the sum of individual line loss which is

$$P_{loss} = \sum_{i=1}^{n} P_{loss,i} \tag{4}$$

2.3. Small Signal Stability Margin and Constraint

In this study, small signal stability margin is related to droop parameters. Higher droop is desired for better power sharing and transient response. The system is said to be stable if the real part of all Eigen values (other than 0) is negative. Small signal stability constraint is thus defined as::

$$R[\lambda_i] < 0,\ \forall\ eigenvalues\ except\ 0 \tag{5}$$

where, λ_i is the i^{th} Eigenvalue of the system and $R[\lambda_i]$ is the real part of that Eigenvalue. Small signal stability limit can be obtained by varying the stability constraints. In this study, droop parameters (m_p and n_q) are taken as system variables. The droop constants are designed using (6) and (7). For the present work, initial values of m_p and n_q are taken as $1.0 \times 10^{-6}\ rpm/W$ and $1.0 \times 10^{-5}\ V/VAR$, respectively.

$$m_{p1} \times P_1 = m_{p2} \times P_2 = ... = m_{pn} \times P_n \tag{6}$$

$$n_{q1} \times Q_1 = n_{q2} \times Q_2 = ... = n_{qn} \times Q_n \quad (7)$$

To perform Eigen value analysis, draw the root locus plot and calculate the losses, we obtain the operating condition/point using time domain simulation or from load flow analysis. Literature on load flow analysis for islanded systems is scarce [33]. The present study preferred time domain simulation using MATLAB/SIMULINK to obtain the operating point. The time domain simulation is also used to validate the Eigen value analysis.

The optimal location of DGs for an IEEE 33-bus radial distributed system presented in [34] is taken as base case for this study. The line and load data for a standard IEEE 33-bus network is available in [35]. Description of the 22-bus practical radial distribution network of APEPDCL is available in [36]-[37].

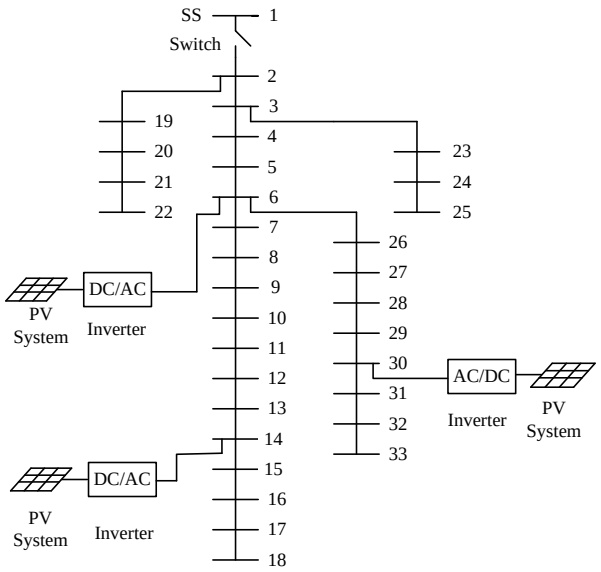

Figure 1: IEEE 33-bus radial distribution system

3. Eigen Value Analysis and Pareto Front Identification

3.1. IEEE 33-bus system with two DGs

The optimal locations of two generators (in a grid-connected system) based on loss minimization proposed in [34] are at nodes 6 and 30. When islanded, these two generators operate in droop control mode (for size in

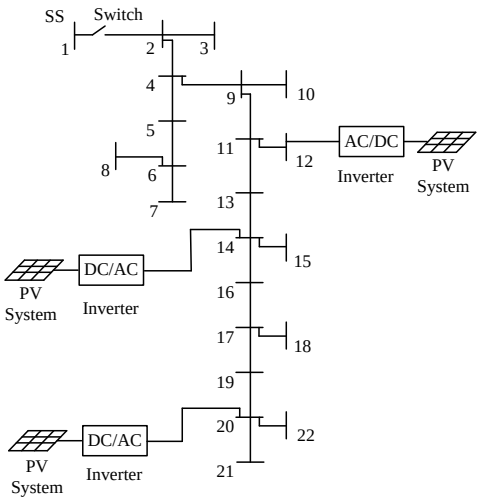

Figure 2: Practical radial distribution (22 bus) network APEPDCL

proportion of 1:0.50) for load sharing. From the droop law, we know that system frequency takes a new steady state value till secondary control acts. System simulation (time domain) is performed with these two generators at various locations (cases) in a standard IEEE 33-bus radial distribution network. From the operating points, state space matrix is obtained using (1). Root locus analysis is performed for these cases by varying the droop constants to identify the stability limit. The values of $m_{p,max}$ and $n_{q,max}$ are noted when the system reaches an unstable region. Losses in the system, minimum voltage value in the total network, $m_{p,max}$, $n_{q,max}$, and minimum distance between the DGs for all these cases are presented in Table 1. It is clear that the maximum values of $m_{p,ma}x$ and $n_{q,max}$ are not the best for case 1. This is true since the decision for placement of generators in this location in [34] was made with separate conditions (grid-connected, exporting power, etc.). However, in systems where grid reliability is poor (true in many developing countries), such location may not be optimum. From network loss, stability, and voltage perspectives, case 1, case 6, and case 13 are preferred options, respectively.

Figure 3 shows the plot between $m_{p,max}$ and Z, while Fig. 4 shows the plot between $n_{q,max}$ and Z for the cases tabulated in Table 1. Electrical distance (in terms of impedance) between generators is an important parameter contributing to small signal stability margin. From Figs. 3 and 4, it is observed that higher electrical distance between sources results in better

Table 1: Various case study results for two DGs placement for IEEE 33-bus radial network

Case	DG-1 Node	DG-2 Node	P_{loss} (kW)	V_{min} (p.u.)	$m_{p,max}$ (10^{-5})	$n_{q,max}$ (10^{-4})	Z (Ω)
1	6	30	65.05	0.9469	1.24	1.34	3.5709
2	24	30	74.27	0.9303	2.30	2.21	7.1671
3	18	24	120.48	0.9193	4.90	5.92	16.8053
4	13	30	264.07	0.9206	3.43	2.84	11.1844
5	18	25	143.45	0.9068	5.33	6.10	17.9422
6	18	22	207.91	0.8855	5.55	6.31	19.6787
7	22	33	185.24	0.9003	3.39	3.84	12.4616
8	22	25	175.09	0.8906	2.08	2.72	7.3835
9	25	33	106.39	0.9131	3.16	3.48	10.7276
10	18	33	386.46	0.8833	5.39	4.58	19.2281
11	6	14	83.96	0.9528	2.44	3.12	8.4827
12	6	18	120.38	0.9524	3.60	5.08	0.9524
13	6	10	72.29	0.9532	1.53	1.97	5.1831
14	3	5	97.04	0.9335	0.88	0.37	0.8118
15	6	26	84.97	0.9487	0.82	0.23	0.2278
16	3	4	103.26	0.9273	0.80	0.27	0.4107
17	9	10	238.42	0.8823	0.73	0.59	1.2764
18	32	33	291.85	0.8507	0.43	0.47	0.6304
19	17	18	525.83	0.7425	0.65	0.50	0.9302
20	24	25	182.31	0.8890	0.66	0.58	1.1377

stability margin. Root locus plot and time domain simulation further prove this point. Case 1 (base case), case 6 (highest stability margin), and case 18 (least stability margin) are considered for detailed analysis.

Figure. 5 shows the root locus plot of the system for case -1, case -6, and case -18. λ_{12} indicates the interaction of low-frequency modes between two sources. From the three sets of Eigen traces, it s clear that the system is going into an unstable region after a certain value of m_P. In Fig. 5, λ_{12} for case -1 starts from -15.066 $\pm$ j 16.60 and reaches the imaginary axis at 0 $\pm$ j 74.40, while for case -6 and case -18 the starting points for λ_{12} are at -15.346 $\pm$ j 1.1835 and -12.971 $\pm$ j 28.278 and they reach the imaginary axis at 0 $\pm$ j 87.05 and 0 $\pm$ j 58.84, respectively. From these root locus plots, the effect of impedance between sources on stability margin is observed, and it is clear that, distance between sources influences the stability of the system.

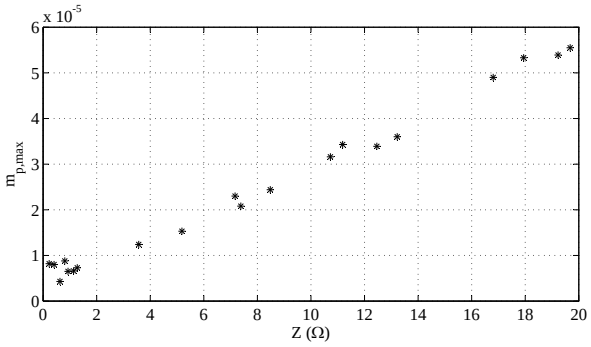

Figure 3: Impedance vs. $m_{p,max}$ plot

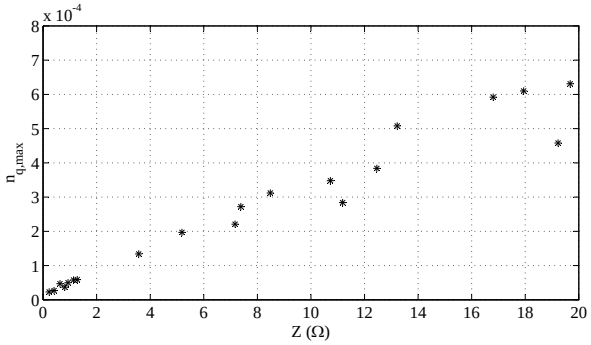

Figure 4: Impedance vs. $n_{q,max}$ plot

3.2. IEEE 33-bus system with three DGs

Optimal locations of three generators (in grid connected system) based on loss minimization, proposed in [34], are at nodes 6, 14, and 30. When islanded, these three generators operate in droop control mode for load sharing. System simulation (time domain) is performed with these three generators at various locations (cases) in a standard IEEE 33 bus radial distribution network. From the operating points, state space matrix is obtained using (1). Root locus analysis is performed for these cases by varying droop constants to identify the stability limit. The values of $m_{p,max}$ and $n_{q,max}$ are noted when the system reaches an unstable region. Losses in the system, minimum voltage value in the total network, $m_{p,max}$, $n_{q,max}$ and minimum distance between the DGs for all these cases are presented in Table. 2.

It is clear that the maximum values of $m_{p,max}$, $n_{q,max}$ are not the highest

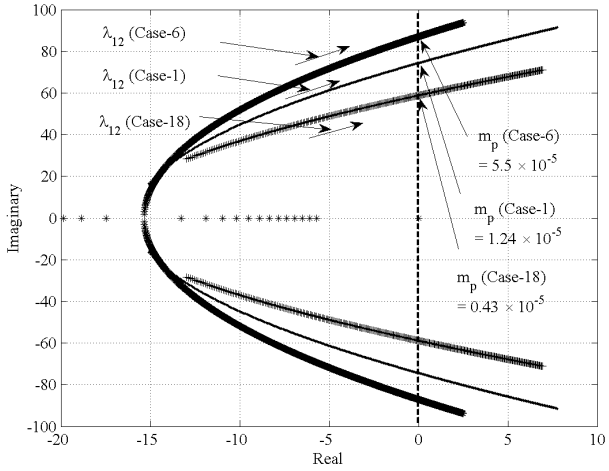

Figure 5: Table 1, cases-1, 6, 18 : Rootlocus plot with variation in droop gain m_p

for case-1. This is true since the decision for this location for placement of generators in this location in [34] was done with separate conditions (grid-connected, exporting power, etc). From network loss, stability, and voltage perspectives, case -37, case -3 and case -33 are preferred options.

Figure. 6 shows the eigenvalues plot for case -1 (base case). Out of 165 eigenvalues 92 eigenvalues are shown in figure (rest of the Eigenvalues are highly damped). For dynamic stability, low-frequency mode Eigenvalues, which are sensitive to the droop gains of the system, are of interest. These low-frequency modes correspond to the power controller mode of the VSI. Case -1 (base case), case -3 (highest stability margin), and case -41 (least stability margin) are considered for detailed analysis. Two complex conjugate low-frequency mode trajectories sensitive to real power droop gain for these cases are shown in Fig. 7, Fig. 8 and Fig. 9, respectively. λ_{12} shows the interaction of low frequency modes between VSIs 1 and 2 while λ_{13} shows the interaction of low frequency modes between VSIs 1 and 3. This trajectory shows that λ_{12} goes into an unstable mode at a lower value of m_p than λ_{13}.

In Fig. 7, λ_{12} starts at -15.7 $\pm$ j 6.2054 and reaches the imaginary axis at 0 $\pm$ 81.265. In Figs. 8 and 9, λ_{12} starts from -15.24 $\pm$ j 8.065 and -11.213 $\pm$ j 33.373 and reaches to imaginary axis at 0 $\pm$ j 86.75 and 0 $\pm$ j 60.118 respectively. From these root locus plots, the impact of minimum distance between sources on stability margin is clearly observed, and it is understood that sources separated with higher impedance have relatively higher stability

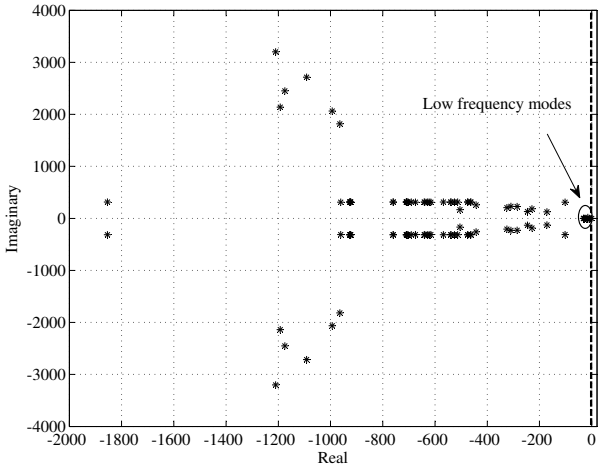

Figure 6: Eigenvalue plot of the microgrid

margin.

Table 2: Various case study results for three DGs placement for IEEE 33-bus radial network

Case	DG-1 Node	DG-2 Node	DG-3 Node	P_{loss} (kW)	V_{min} (p.u.)	$m_{p,max}$ (10^{-5})	$n_{q,max}$ (10^{-4})	Z_{min} (Ω)
1	6	30	14	60.03	0.9581	1.81	1.31	3.5709
2	25	33	18	67.98	0.9635	2.91	4.12	10.7274
3	22	33	18	86.76	0.9441	2.94	4.73	12.4616
4	24	30	8	32.36	0.9694	0.92	1.80	6.1455
5	24	30	18	44.86	0.9751	2.38	2.62	7.1671
6	6	30	18	79.30	0.9577	1.78	1.38	3.4992
7	24	30	6	45.94	0.9530	0.53	0.76	3.5965
8	24	30	22	52.07	0.9364	1.35	2.05	6.2483
9	24	6	18	84.58	0.9613	1.22	1.29	3.5965
10	10	30	15	126.06	0.9347	1.19	1.31	4.0902
11	10	24	15	153.56	0.9360	1.18	1.30	4.0902
12	10	22	15	151.49	0.9167	1.19	1.35	4.0902
13	24	30	20	45.87	0.9370	1.08	1.50	4.4788
14	24	20	18	95.61	0.9321	1.80	1.84	4.4788
15	24	30	3	46.11	0.9471	0.54	0.57	1.6905
16	24	3	18	75.06	0.9422	0.44	0.16	1.6905
17	24	21	3	135.0	0.9235	0.43	0.53	1.6905
18	24	22	18	114.78	0.9299	2.23	2.62	6.2483
19	6	11	18	212.26	0.9554	0.94	1.71	5.3783
20	2	6	18	65.20	0.9617	1.07	0.97	2.456
21	24	21	2	139.08	0.9181	0.40	0.59	2.2352
22	2	6	30	36.66	0.9528	0.61	0.79	2.456
23	24	21	6	96.28	0.9509	0.82	1.04	3.5965
24	8	14	18	362.75	0.9062	0.62	1.46	4.7548
25	2	4	6	76.63	0.9514	0.41	0.42	0.964
26	24	21	11	91.14	0.9409	1.63	2.01	5.0983
27	7	26	30	64.41	0.9514	0.64	0.26	0.8209
28	10	14	18	386.80	0.8604	0.60	1.16	3.2999
29	3	6	11	41.92	0.9627	0.72	0.77	2.3629
30	3	6	30	34.80	0.9532	0.60	0.72	2.3629
31	24	21	14	85.60	0.9363	1.83	2.08	5.0983
32	24	30	11	25.81	0.9770	1.48	2.68	7.1429
33	23	30	18	51.56	0.9779	2.31	2.25	6.0099
34	23	33	18	77.61	0.9746	2.84	3.22	15.6619
35	23	19	3	112.85	0.9244	0.37	0.25	0.5472
36	6	12	18	231.84	0.9552	0.82	1.70	5.7461
37	24	30	14	25.69	0.9759	1.94	2.64	7.1671
38	23	3	4	100.50	0.9301	0.43	0.25	0.4170
39	19	2	3	130.38	0.9224	0.41	0.27	0.2267
40	5	6	26	67.69	0.9532	0.43	0.21	0.2278
41	29	30	31	193.0	0.8980	0.33	0.34	0.6214
42	24	23	3	119.09	0.9236	0.37	0.31	0.5472
43	21	20	19	246.34	0.9051	0.42	0.45	0.6297
44	4	6	8	52.80	0.9630	0.44	0.64	1.5007
45	28	30	32	175.37	0.9153	0.35	0.61	1.6249
46	10	11	12	295.94	0.8632	0.50	0.22	0.2071

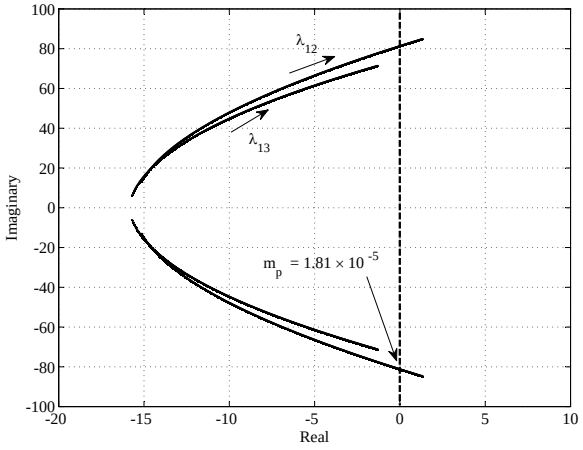

Figure 7: Table 2, case-1 : Rootlocus plot with variation in droop gain m_p

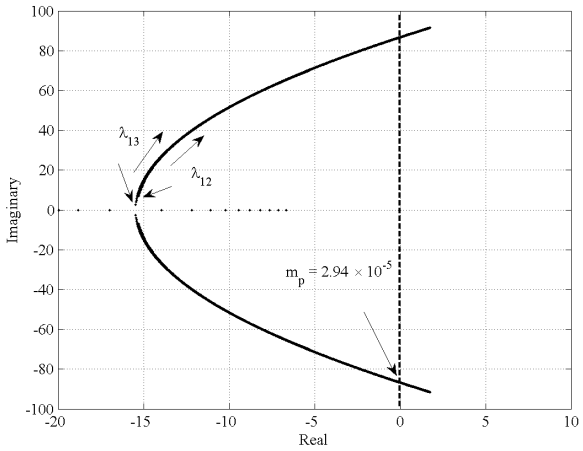

Figure 8: Table 2, case-3 : Rootlocus plot with variation in droop gain m_p

3.3. 22-bus APEPDCL Distribution Network

The optimal locations of three generators (in a grid-connected system) based on loss minimization, proposed in [36], are at nodes 12, 14, and 20. System simulation (time domain) is performed with these three generators at various locations (cases) in the 22-bus APEPDCL distribution network. From the operating points, state space matrix is obtained using (1). Root

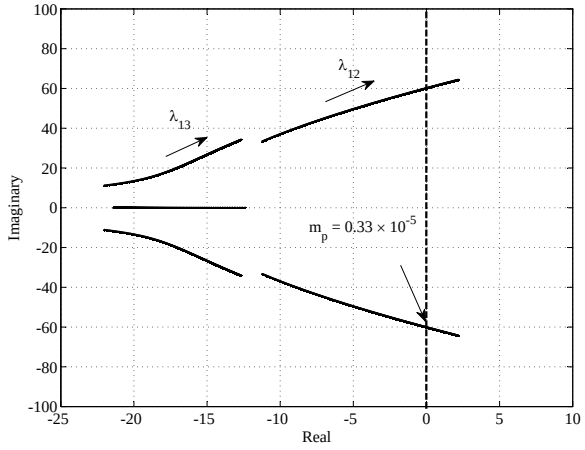

Figure 9: Table 2, case-41 : Rootlocus plot with variation in droop gain m_p

locus analysis is performed for these cases by varying droop constants to identify the stability limit. The values of $m_{p,max}$ and $n_{q,max}$ are noted when the system reaches an unstable region. Losses in the system, minimum voltage value in the total network, $m_{p,max}$, $n_{q,max}$, and minimum distance between the DGs for all these cases are presented in Table. 3.

It is clear that the maximum values of $m_{p,max}$, $n_{q,max}$ are not the highest for case 1. This is true since the decision for placement of generators in this location was made with separate conditions (grid-connected, exporting power, etc.). From network loss, stability, and voltage perspectives, case 8, case 6, and case 8 are preferred options. Case 1 (base case), case 6 (highest stability margin) and case 20 (least stability margin) are considered for detailed analysis.

Table 3: Various case study results for three DGs placement for APEPDCL 22-bus practical radial network

Case	DG-1 Node	DG-2 Node	DG-3 Node	P_{loss} (kW)	V_{min} (p.u.)	$m_{p,max}$ (10^{-6})	$n_{q,max}$ (10^{-5})	Z_{min} (Ω)
1	12	14	20	0.740	0.9952	7.23	4.48	1.2137
2	3	14	20	0.752	0.9967	7.29	4.90	1.2137
3	8	12	22	3.154	0.9951	12.06	8.49	3.6752
4	8	13	22	2.627	0.9958	11.01	8.04	3.0911
5	4	15	22	0.612	0.9971	8.41	6.10	1.8402
6	8	10	22	4.4459	0.9942	13.01	8.16	2.9157
7	3	15	22	0.953	0.9965	8.45	6.25	1.8402
8	4	14	20	0.367	0.9972	7.26	4.85	1.1897
9	9	15	22	0.732	0.9968	8.33	5.76	1.8402
10	8	9	17	5.078	0.9965	10.32	7.10	2.8026
11	3	10	17	3.675	0.9965	10.04	5.60	1.5681
12	8	11	17	3.586	0.9967	8.95	6.49	2.0428
13	8	10	18	5.041	0.9961	10.66	7.47	2.9157
14	12	15	18	0.943	0.9953	5.91	3.49	0.5567
15	15	18	22	2.712	0.9903	7.60	3.50	0.5567
16	10	12	15	2.050	0.9954	8.06	4.11	0.8826
17	13	14	15	1.514	0.9945	6.02	2.13	0.0249
18	20	21	22	6.410	0.9840	6.43	2.17	0.0980
19	9	10	11	5.281	0.9879	6.61	2.16	0.0615
20	6	7	8	19.336	0.9683	5.83	2.15	0.0673

Plots of $m_{p,max}$ vs. Z_{min} (minimum impedance among sources) and $n_{q,max}$ vs. Z_{min} are shown in Figs. 10 and 11, respectively.

Figures. 12, 13 and 14 show root locus plot for cases 6, 8 and 20, respectively. λ_{12} shows the interaction of low-frequency modes between VSIs 1 and 2 while λ_{13} shows the interaction of low frequency modes between VSIs 1 and 3. This trajectory shows that λ_{12} goes into an unstable mode at a lower value of m_p than λ_{13}. In Fig. 12 λ_{12} starts from an approximate value of -15.55 $\pm$ j 21.27 and reaches the imaginary axis at an approximate value of 0 $\pm$ j 63.3. In Figs. 13 and 14, λ_{12} approximately starts from -15.27 $\pm$ j 15.275 and -16.19 $\pm$ j 24.70 and reaches the imaginary axis approximately at 0 $\pm$ j 71.1 and 0 $\pm$ j 59.7 respectively. The following are some critical observations from the case studies:

- The system configuration (generator location) with low losses in grid

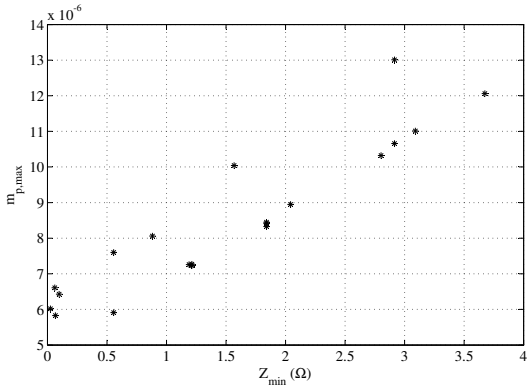

Figure 10: Plot between $m_{p,max}$ vs. Z_{min}

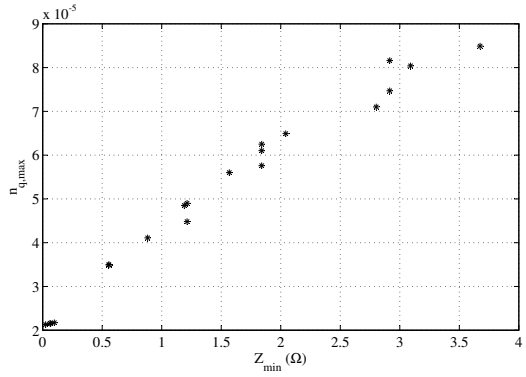

Figure 11: Plot between $n_{q,max}$ vs. Z_{min}

connected mode may suffer from stability issues when islanded. This can be a serious problem when the reliability of the main grid is poor.

- The interaction of low-frequency modes between various DGs is different and the location of some inverters is critical (inverter 2 in this case) with respect to the stability.
- Stability margin (gain of droop constant) is a function of minimum distance between the generators in an islanded network.
- It is important to choose an optimal location for these generators by considering stability and network losses.

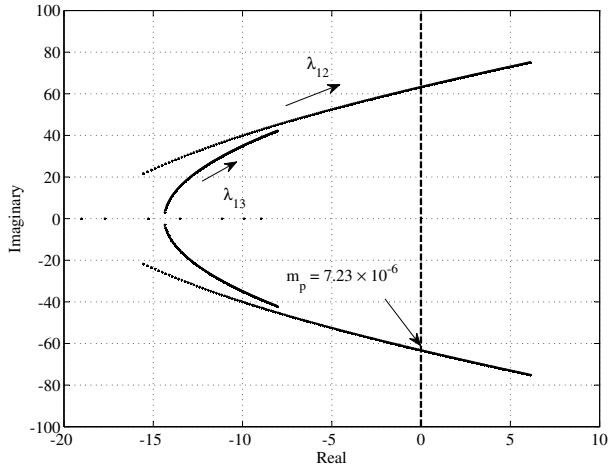

Figure 12: Table 3, case-1 : Rootlocus plot with variation in droop gain m_p

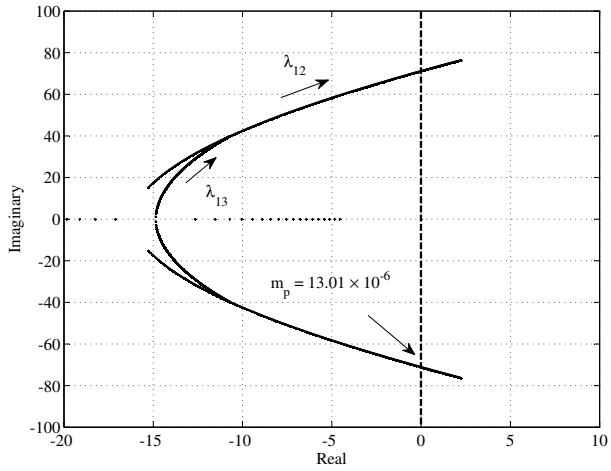

Figure 13: Table 3, case-6 : Rootlocus plot with variation in droop gain m_p

3.4. Determination of Pareto Front in an Islanded Microgrid

The locations of generators should depend on network losses and overall stability of the system. For multi-objective optimization of the DG network, Pareto optimal front should be identified. Data in Tables 2 and 3 are plotted and Pareto fronts (set of non dominated solutions) obtained between $m_{p,max}$ vs. real power loss and $n_{q,max}$ vs. reactive power loss (Figs. 15, 16 and 17, 18 respectively).

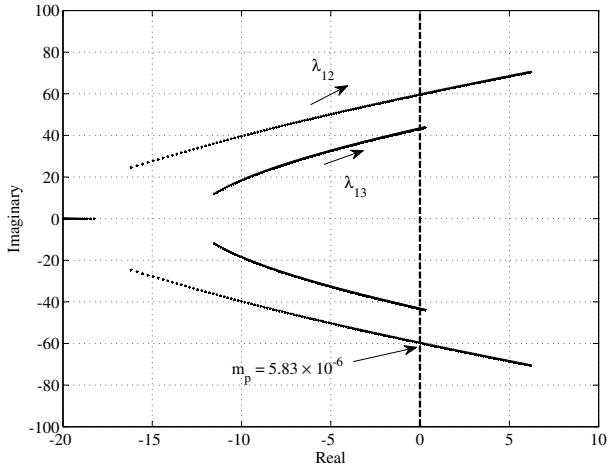

Figure 14: Table 3, case-20 : Rootlocus plot with variation in droop gain m_p

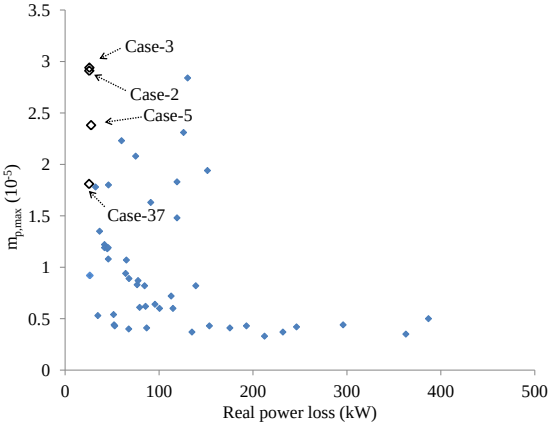

Figure 15: Real power loss vs. $m_{p,max}$ for IEEE 33 bus system with three DGs - Pareto front shown in open boxes

Critical observations from Pareto fronts (for 33-bus system) are:

- Cases corresponding to Pareto fronts (shown in open box) obtained in Fig. 15 are 2, 3, 5 and 37.
- Cases corresponding to Pareto fronts (shown in open box) obtained in Fig. 16 are 2, 3 and 32.

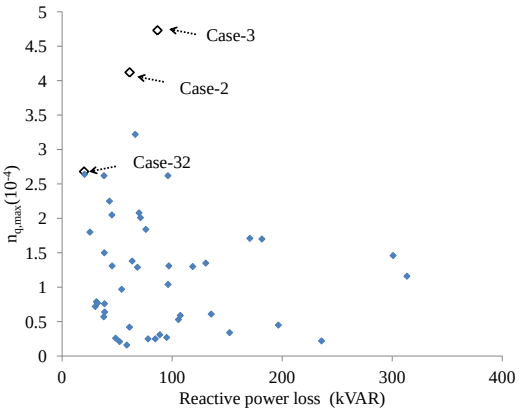

Figure 16: Reactive power loss vs. $n_{q,max}$ for IEEE 33 bus system with three DGs - Pareto front shown in open boxes

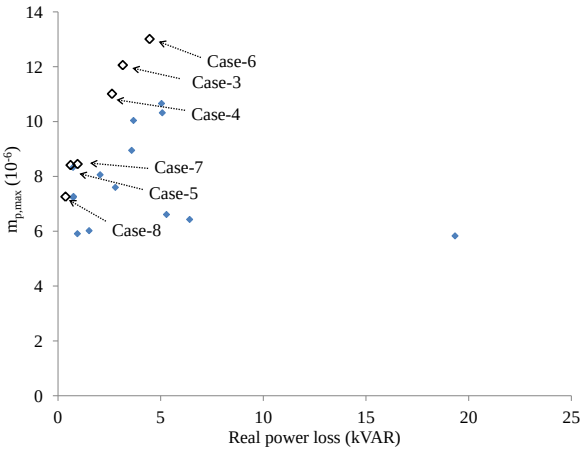

Figure 17: Real power loss vs. $m_{p,max}$ for 22 bus APEPDCL network with three DGs - Pareto front shown in open boxes

- Case-1 which represents optimal location of sources in a grid-connected system, does not lie on the Pareto front. This clearly indicates that the optimal placement of sources in a grid-connected microgrid is not optimal during islanding.

Critical observations from Pareto fronts (for 22 bus practical system) are:

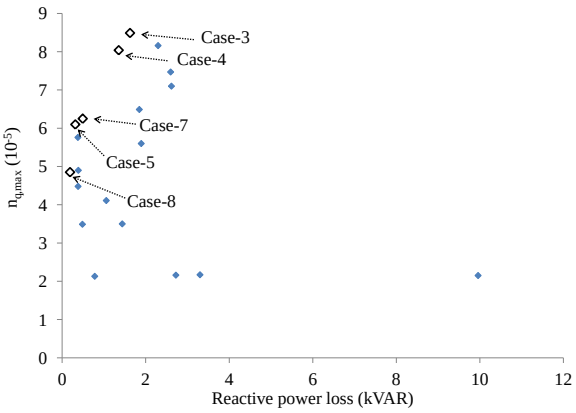

Figure 18: Reactive power loss vs. $n_{q,max}$ for 22 bus APEPDCL network with three DGs - Pareto front shown in open boxes

- Cases corresponding to Pareto fronts (shown in open box) obtained in Fig. 17 are 3, 4, 5, 6, 7 and 8.
- Cases corresponding to Pareto fronts (shown in open box) obtained in Fig. 18 are 3, 4, 5, 7 and 8.
- Similar to the previous example, case -1 does not lie on the Pareto front.
- Cases 3, 4, and 6 have high stability margin and higher losses, while cases 5, 7, and 8 have low stability margin and low losses.

4. Simulation - Time Domain Validation

Time domain simulation is performed on both the networks for validation of stability analysis. Simulation results for the three DG system (case -1 of Table 2) and for the practical network (case -1 of Table. 3) are shown in Fig. 19 and Fig. 20, respectively.

The system is stable and sharing power as per the droop law. The effect of higher value of droop parameter is investigated by changing the droop value (beyond $m_{p,max}$). At time t = 2s for a higher value of m_p ($> m_{p,max}$), power output of DGs is oscillating with increasing amplitude as shown in Fig. 19, which indicates that the system is now unstable.

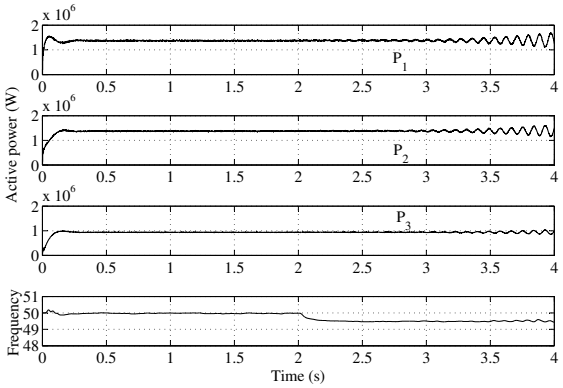

Figure 19: Real power output of DGs and system frequency in Std. IEEE 33 network

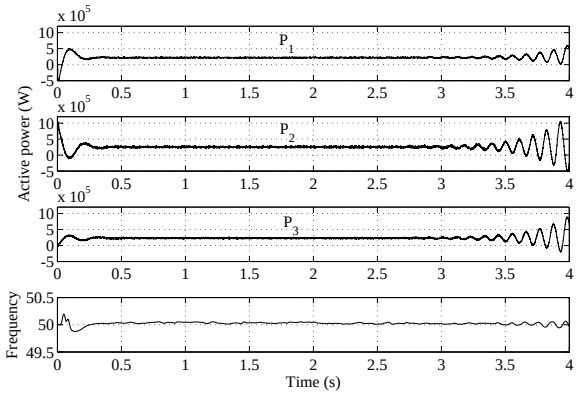

Figure 20: Real power output of DGs and system frequency in practical 22 bus distribution network

5. Conclusion

The effect of location of droop-based sources on small signal stability, transient response, and network losses in an islanded network is investigated. A standard IEEE 33-bus network and a 22-bus practical distribution network are chosen. A microgrid model is developed for both the networks with droop-based sources, network components, and loads for stability analysis. Higher droop in DGs is desired for better power sharing and transient response. Small signal stability is studied for various locations of DGs (two/three) by varying the droop constant. From the stability study, it is found that a system optimized for losses in grid-connected mode may suffer from small signal

stability issues and poor transient response when in islanded configuration. The minimum distance between generators in the network also has an impact on small signal stability. For multi-objective optimization of the DG network, Pareto optimal front is identified. Results of small signal stability analysis are verified using time domain simulation in MATLAB for both the networks.

References

[1] M. Thomson, and D. G. Infield, Impact of widespread photovoltaics generation on distribution systems, IET Renew. Power Gene. 1(1)(2007)33-40.

[2] N. L. Soultanis, S. A. Papathanasiou, and N. D. Hatziargyriou, A Stability Algorithm for the Dynamic Analysis of Inverter Dominated Unbalanced LV Microgrids, IEEE Trans. Power Syst. 20(1)(2007)294-304.

[3] P. S. Georgilakis, and N. D. Hatziargyriou, Optimal distributed generation placement in power distribution networks: models, methods, and future research, IEEE Trans. Power Syst. 28(3)(2013)3420-3428.

[4] H. L. Willis, Analytical methods and rules of thumb for modeling DG distribution interaction, in Proc. IEEE Power Eng. Soc. Summer Meeting (2000)1643-1644.

[5] N. Acharya, P. Mahat, and N. Mithulananthan, An analytical approach for DG allocation in primary distribution network, Int. J. Elect. Power Energy Syst. 28(10)(2006)669-678.

[6] D. Q. Hung, and N. Mithulananthan, Loss reduction and loadability enhancement with DG: A dual-index analytical approach, Appl. Energy 115(2014) 233-241.

[7] X. Fua, H. Chena, R. Caic, and P. Yang, Optimal allocation and adaptive VAR control of PV-DG in distribution networks, Appl. Energy, 137(1)(2015) 173-182.

[8] D. Q. Hung, N. Mithulananthan, and R.C. Bansal, Analytical strategies for renewable distributed generation integration considering energy loss minimization, Appl. Energy 105(2013) 75-85.

[9] W. Sheng, K. Liu, X. Meng, X. Ye, and Yongmei Liu, Research and practice on typical modes and optimal allocation method for PV-Wind-ES in Microgrid, Elect. Power Syst. Res. 120(10)(2015)242-255.

[10] E.E. Sfikas, Y.A. Katsigiannis, and P.S. Georgilakis, Simultaneous capacity optimization of distributed generation and storage in medium voltage microgrids, Electr. Power Syst. Res. 67(2015)101-113.

[11] M. H. Moradia, M. Eskandarib, and H. Showkatia, A hybrid method for simultaneous optimization of DG capacity and operational strategy in microgrids utilizing renewable energy resources, Electr. Power and Energy Syst. 56(3)(2014) 241-258.

[12] A. Khodaei, Microgrid optimal scheduling with multi-period islanding constraints, IEEE Trans. Power Syst. 29(3)(2014) 1383-1392.

[13] S. Conti, R. Nicolosi, S. A. Rizzo, and H. H. Zeineldin, Optimal dispatching of distributed generators and storage systems for MV islanded microgrids, IEEE Trans. Power Del. 27(3)(2012),1243-1251.

[14] S. J. Ahn, S. R. Nam, J. H. Choi, and S. Moon, Power scheduling of distributed generators for economic and stable operation of a microgrid, IEEE Trans. Smart Grid 4(1)(2013) 398-405.

[15] M. Gomeza, A. Lopezb, and F. Juradoa, Optimal placement and sizing from standpoint of the investor of photovoltaics grid-connected systems using binary particle swarm optimization, Appl. Energy, 87(6)(2010) 1911-1918.

[16] H. Rena, W. Zhoub, K. Nakagamib, W. Gaoc, and Q. Wuc, Multi-objective optimization for the operation of distributed energy systems considering economic and environmental aspects, Appl. Energy, 87(12)(2010) 3642-3651.

[17] T. Niknama, S. I. Taheria, J. Aghaeia, S. Tabatabaeib, and M. Nayeripoura, A modified honey bee mating optimization algorithm for multiobjective placement of renewable energy resources, Appl. Energy, 88(12)(2011) 4817-4830.

[18] M. M. A. Abdelaziz, and E.F. El-Saadany, Maximum loadability consideration in droop-controlled islanded microgrids optimal power flow, Electr. Power Syst. Res., 10(6)(2014) 168-179.

[19] M. M. A. Abdelaziz, E. F. El-Saadany, and R. Seethapathy, Assessment of droop-controlled islanded microgrid maximum loadability, IEEE PES general meeting (2013)1-5.

[20] M. M. A. Abdelaziz, and E. F. EI-Saadany, Determination of worst case loading margin of droop-controlled islanded microgrids, IEEE International Conference on Electric Power and Energy Conversion Systems (EPECS) (2013)1-6.

[21] A. Soroudi, and M. Ehsan, IGDT based robust decision making tool for DNOs in load procurement under severe uncertainty, IEEE Trans. Smart Grid 4(2)(2013)886-895.

[22] M. M. A. Abdelaziza,and E.F. El-Saadanyb, Economic droop parameter selection for autonomous microgrids including wind turbines, Renewable Energy (2014)393-404.

[23] B. Yan, B. Wang, F. Tang, D. Liu, Z. Ma, and Y. Shao, Development of economics and stable power-sharing scheme in autonomous microgrid with volatile wind power generation, Elect. Power Comp. and Syst. 42(12)(2014),1313-1323.

[24] X. Wu, C. Shen, M. Zhao, Z. Wang, and X. Huang, Small signal security region of droop coefficients in autonomous microgrids, IEEE PES general meeting (2014)1-5.

[25] E. Barklund, N. Pogaku, M. Prodanvoic, C. Hernandez- Aramburo, and T. C. Green, Energy management in autonomous microgrid using stability-constrained droop control of Inverters, IEEE Trans. Power Electron. 23(5)(2008)2346-2352.

[26] F. Katiraei, M. R. Iravani, and P. W. Lehn, Small-signal dynamic model of a microgrid including conventional and electronically interfaced distributed resources, IET Gener. Transmiss. Distr. 1(3)(2007)369-378.

[27] G. Dfaz, C. G. Moran, J. G. Aleixandre, and A. Diez, Scheduling of droop coefficients for frequency and voltage regulation in isolated microgrids, IEEE Trans. Power Syst. 25(1)(2010)489-496.

[28] A. D. Paquette, M. J. Reno, R. G. Harley, and D. M. Diwan, Transient load sharing between inverters and synchronous generators in islanded microgrids, IEEE Energy Conversion Congress and Exposition (ECCE) (2012)2735-2742.

[29] M. A. Hassan, and M. A. Abido, Optimal design of microgrids in autonomous and grid-connected modes using particle swarm optimization, IEEE Trans. Power Electron. 26(3)(2011)755-769.

[30] I. Y. Chung, W. Liu, D. A. Cartes, E. G. Collins, and S. I. Moon, Control methods of inverter-interfaced distributed generators in a microgrid system, IEEE Trans. Ind. Appl. 46(3)(2010)1078-1088.

[31] S-J. Ahn, J-W. Park, I-Y. Chung, S-I. Moon, S-H. Kang, and S-R. Nam, Power sharing method of multiple distributed generators considering control modes and configurations of a microgrid, IEEE Trans. Power Del. 25(3)(2010)2007-2016.

[32] N. Pogaku, M. Prodanovic, and T. C. Green, Modeling, analysis and testing of autonomous operation of an inverter-based microgrid, IEEE Trans. Power Electron. 22(2)(2007) 613-625.

[33] M. M. A. Abdelaziz, H. E. Farag, E. F. El-Saadany, and Y. A. R. I. Mohamed, A novel and generalized three-phase power flow algorithm for islanded microgrids using a Newton Trust Region method, IEEE Trans. Power Syst. 28(1)(2013)190-201.

[34] D. Q. Hung, and N. Mithulananthan, Multiple distributed generator placement in primary distribution networks for loss reduction, IEEE Trans. Ind. Elect. 60(4)(2013) 1700-1708.

[35] B. Venkatesh, R. Ranjan, and H. B. Gooi, Optimal reconfiguration of radial distribution systems to maximize loadability, IEEE Trans. Power Syst. 19(1)(2004)260-266.

[36] I. S. Kumar, Implementation of nature inspired meta-heuristic algorithms to optimal allocation of distributed generators in radial distribution systems, Ph.D thesis, JNTU Kakinada, AP, India, 2015.

[37] M. R. Raju, K.V.S. R. Murthy, and K. Ravindra, Direct search algorithm for capacitive compensation in radial distribution systems, Electr. Power and Energy Syst. 42(1)(2012)24-30.